Nucleation and detachment of polystyrene nanoparticles from plowing-induced surface wrinkling

Jana Hennig [a], Alexander Litschko [a], Juan J. Mazo [b,c], Enrico Gnecco [a,d,*]

[a] Otto Schott Institute of Materials Research (OSIM), Friedrich Schiller University Jena, 07743 Jena, Germany
[b] Departamento de Física de la Materia Condensada, Universidad de Zaragoza, 50009 Zaragoza, Spain
[c] Instituto de Nanociencia y Materiales de Aragón (INMA), CSIC-Universidad de Zaragoza, 50009 Zaragoza, Spain
[d] Center for Energy and Environmental Chemistry Jena (CEEC Jena), Friedrich Schiller University Jena, 07743 Jena, Germany

ARTICLE INFO

ABSTRACT

We report the formation of spherical particles (up to 250 nm in diameter) from polystyrene surfaces repeatedly scratched by atomic force microscopy nanotips (nominal radius < 10 nm) along a series of parallel lines. The particles nucleate from the crests of the ripple profiles formed in the beginning of the scratch process. They are subsequently detached and progressively displaced by the tip across the ripples till the edge of the scanned area, where they pile up without coalescing. The detachment occurs smoothly without static friction peaks, suggesting that the particles are torn off as a result of a crazing mechanism induced by the tip when it is pushed against the ripple crests. Considering the negative impact of nanoplastics on the environment and human health, and the absence of established methodologies for a quantitative analysis of these processes at the level of single particles, our results will help to promote systematic characterization of plowing wear on different polymeric materials and different environmental conditions.

1. Introduction

Environmental pollution by polymer waste is an issue of utmost importance nowadays. By a combination of different factors, like mechanical stress, UV radiation and water, macroscopic plastic fragments routinely degrade into micro- and nanoplastics [1]. The tiny particles so produced cause serious problems for the environment and for human health. They are difficult to localize and cleared away, and, due to their size, they are easily transported by air and water on very large distances [2-4]. Since the particles can be ingested by organisms at the base of food-chain, they end up being extremely harmful also for human beings [5, 6]. Inside the organism they create threats caused by their physical size and chemical composition [7]. For these reasons there is no doubt that pollution caused by the release of micro- and especially of nanoplastics into the environment has to be monitored and reduced, but our knowledge on this topic is currently very limited [8]. Especially the individual nucleation and release of polymer nanoparticles accompanying abrasive processes has been rarely investigated from the physical point of view, which is mainly due to the characteristic length scales of these processes.

Here we present a quantitative investigation of plowing wear on polystyrene (PS) surfaces as performed by atomic force microscopy (AFM) in ambient conditions. The same instrument has been used for both scraping and imaging the damaged material. Polystyrene was chosen since it is one of the most common plastic materials, meaning that large amounts of PS nanoparticles are found all over the Earth planet [9]. It is also very stable and extremely hard to degrade in the environment [10], which makes it one of the most problematic materials to deal with in environmental protection. The paper is organized as follows: After comparing AFM topographies of the damaged area recorded during and after scratching the surfaces, we focus on the extrusion, detachment and displacement of the PS nanoparticles and recognize crazing caused by the AFM tip as the key mechanism at the basis of the nucleation process. This mechanism acts on the background of the wavy (ripple) patterns formed in the very first scratch, which have been repeatedly discussed in the literature [11-18].

2. Results and discussion

Rippling of compliant surfaces scraped by a nanotip is associated to the elastic instabilities periodically reached by the tip, which indents the surface material while it is driven laterally [17]. If the tip follows a series

---

of parallel scan lines only in one direction (e.g. left to right) the resulting ripples are oriented in two directions: either parallel to the side edges of the scanned area (*boundary region*) or tilted by an angle θ with respect to the scan (*x*) direction (*steady region*) [18]. The angle θ tends to increase with the distance *b* between consecutive scan lines. These results have been reproduced by numeric simulations based on an extension of the Prandtl model for atomic-scale friction with a variable interaction potential corresponding to the evolving surface profile [19]. However, the observation of fine structures developed out of the ripple crests is difficult if the same tip is used to form and image the surface ripples. For this reason, we have scratched the PS surfaces in contact mode, and imaged the resulting structures in tapping mode using supersharp tips with nominal radius below 7 nm. Nanoscratch tests were repeated several times on the same regions of the sample surfaces.

A series of topography images recorded while scratching an initially flat surface up to five times is presented in Fig. 1(a-c). Only the last scan in each series is shown. Figure 1(a) perfectly matches the results presented by Mazo *et al.* [18]. Ripples are formed all over the scanned area. In the steady region they are oriented, on the average, by an angle θ = 55° and their period is about 200 nm. Imaging the rippled surfaces in tapping mode, as shown in Fig. 1(d-f), allowed us to resolve structures which are not visible in the images recorded while scratching. In Fig. 1(e) spherical asperities start to nucleate on the ripple crests. Their diameter does not exceed 250 nm. Several spheres are also detached from their original location and piled up along both edges of the scanned area, as clearly visible when zooming out: see Fig. 2(a). In Fig. 1(f) the process goes on with the nucleation of more spheres. The sphere diameters increase on the average, but they never exceed 250 nm. Note that the spheres keep their identity in the pile-ups, as clearly seen in the left part of Fig. 1(f) with enhanced negative contrast (these spheres are generated when the tip comes back and indents the surface again). The root mean square (RMS) surface roughness measured in the steady regions in Figures 1(d-f) is 15.7, 11.5 and 18.1 nm respectively, see Fig. 2 (c). It means that the ripple pattern is partially smoothed when the particles are released, and it is roughened again as the nucleation and

removal processes are repeated. In contrast, the RMS roughness measured in contact mode does not show any decrease, as also seen in Fig. 2(c). It is also lower than the RMS in tapping mode. Similar trends have been observed in other series of scratch tests performed with a different tip and more data points (up to ten: see Supp. Figures S1-S3).

To understand the results obtained after the first scan (Fig. 1a) we start from the interpretation given by Mazo *et al.* [18]. The AFM tip indents the surface viscoplastically and, at the same time, it extrudes the polymer material all around the indentation pit, as sketched in Fig. 3(a). As the tip is driven to the right by the cantilever spring holding it (not shown) more material is pushed up until the mechanical equilibrium of the system becomes unstable, and the tip slips across the crest on its right. When the process is repeated along parallel scan lines it results in the ripples oriented by an angle θ < 90°. Note that in Ref. [18] the volume under the surface profile (dashed red curve) was assumed to remain constant during the scratch process. This hypothesis was based on nanoindentation tests performed on a PS surface without scratching [17] and, as mentioned before, it allowed us to explain not only the formation of oblique ripples in the steady regions but also of ripples parallel to the (left) edge of the scanned regions. However, the first cross-section on the bottom of Fig. 2(c) clearly shows that the apparent volume above the initially flat surface is larger than the volume extruded by the tip. Since the nominal radius of the tip used in tapping mode (< 7 nm) is well below the radius of curvature of the valleys (~100 nm) the difference cannot be explained by the convolution between tip and surface profiles only [20]. In any case, the model is not devised to predict (in the present form) the formation and detachment of the nanospheres.

The disagreement can be overcome by assuming that (i) the polymer surface partially recovers when the normal stress exerted in contact mode is released [21] and (ii) the ripple profiles pushed by the tip undergo *crazing* [22, 23], as schematically shown in Fig. 3(b). The crazing mechanism is typical of amorphous thermoplastics loaded in tension slightly below the glass temperature. In that case, microgaps are formed in a plane normal to the stress. The gaps are bridged by fibrils of only few
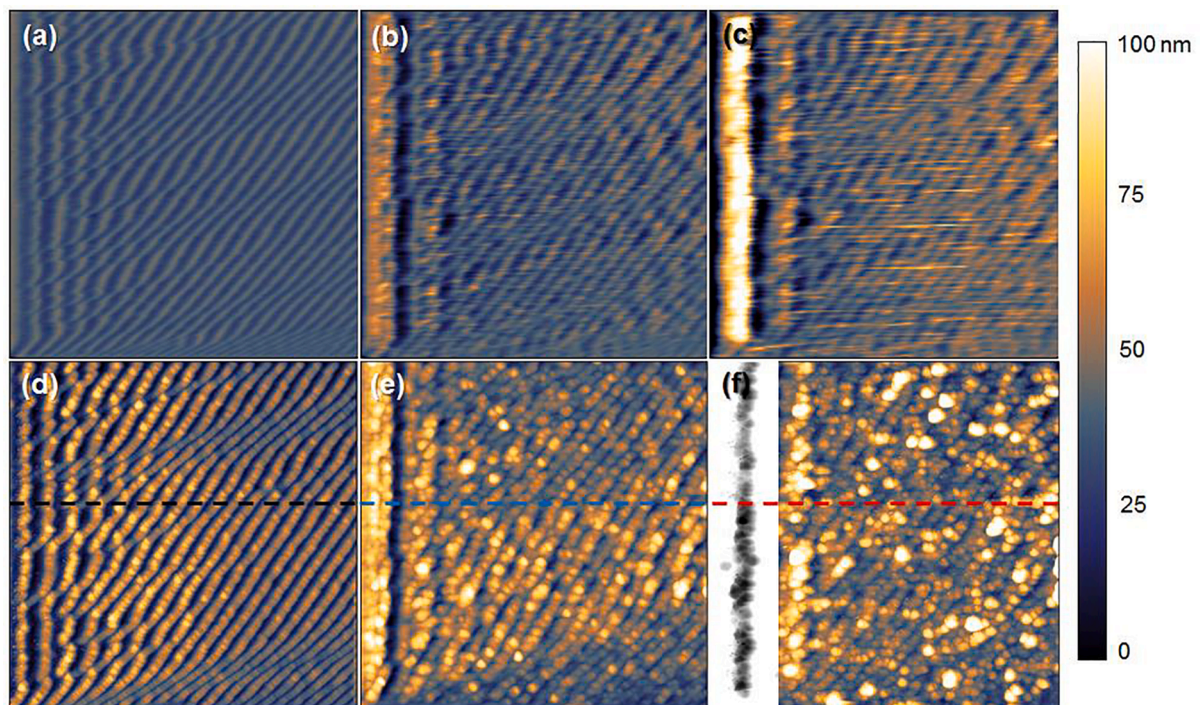

Fig. 1. Topography images acquired while scraping different areas of an initially flat polystyrene surface with $F_N = 100$ nN, v = 15 μm/s and b = 20 nm (a) once, (b) 3 times and (c) 5 times. Frame sizes: 5×5 μm^2. (d-f) Corresponding images of the damaged areas acquired in tapping mode afterwards (the pile-up on the left edge of the area scratched 5 times being shown with negative contrast).
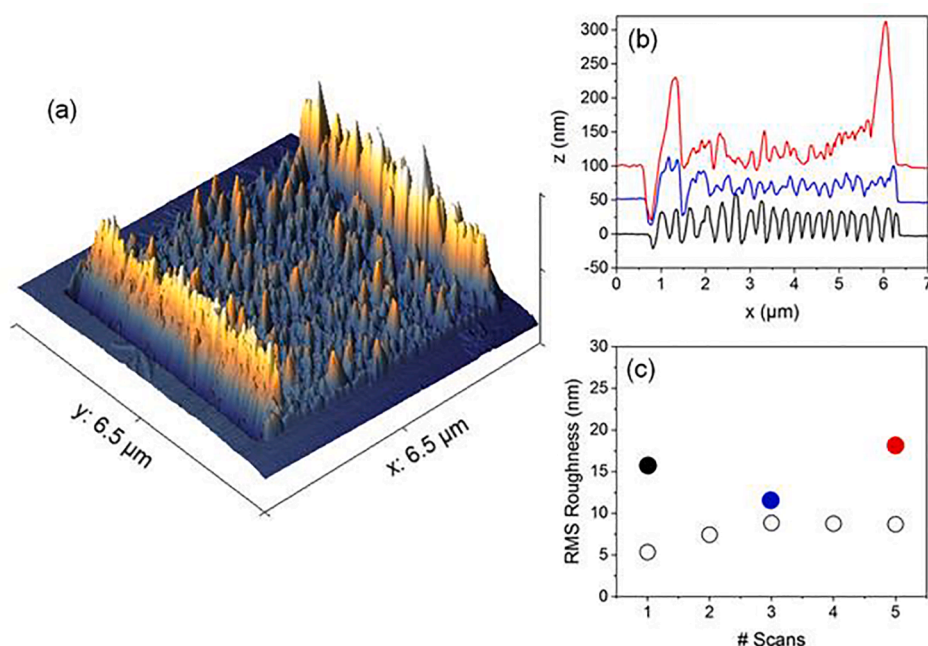
Fig. 2. (a) Enlarged 3D view of a region encompassing the area in Fig. 1f (vertical bar = 330 nm). (b) Black, blue and red cross-sections corresponding to the dashed lines in Fig. 1d, 1e and 1 f respectively with 1 μm added on both left and right edges and different offsets introduced for sake of clarity. (c) RMS roughness on 2×2 μm^2 areas in the steady regions imaged in contact mode while scratching the PS surface (open circles) and in tapping mode afterwards (filled circles, same color assignment as in Fig. 2b).
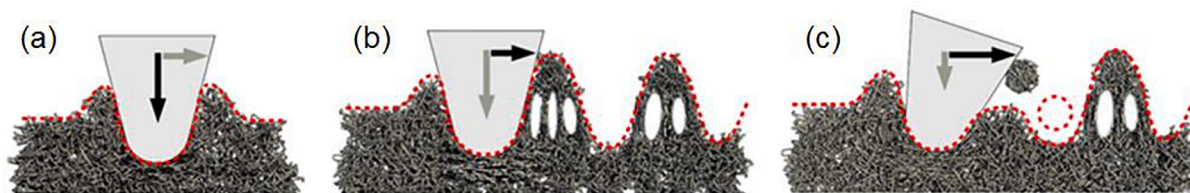

Fig. 3. Three phases of the proposed mechanism for particle formation and detachment: (a) Extrusion of material all around the location initially indented by the AFM tip; (b) Crazing process and particle nucleation caused by the increasing lateral force on a (previously formed) ripple pattern; (c) Sphere detachment.

nm in diameter, which become longer and narrower as the tension increase, until they start breaking. In the present case, the polymer chains in the extruded regions are stretched and voids are formed, which leads to an apparent increase of the volume below the surface profile. The effect is expected to appear first on the right side of the indentation pit, where a time-increasing shear stress is added to the normal stress. When the tensile strength value $\tau = 35\text{-}55$ MPa of polystyrene is reached [24], the asperities are detached in the form of nanospheres whose size is necessarily limited by the radius of curvature R of the ripple crests (in the order of 100 nm). Assuming that the radius of the last "neck" being cut in Fig. 3(b) is well below R, visible lateral force variations are not expected when the particle detachment occurs. For instance, with a radius in the order of 0.5 nm, the shear force required to cut the neck would be in the order of 50 pN (since the shear strength is about 50 MPa). This is well below the lateral force values of few hundred nN which are typically observed in the rippling process [16]. Once a PS nanosphere is removed, the remaining part of the ripple crest is made available for the nucleation of new spheres in the next scans; see Fig. 3 (c). Note that the role of crazing in the rippling process of polymer surfaces was already hypothesized by Schmidt *et al.* [13] although the formation of wear particles was not reported in their work.

The manipulation of the nanospheres across the ripple pattern is also worth to be discussed. Gnecco *et al.* [25] observed that, when AFM is used to manipulate rigid (gold) nanospheres across a rigid (glass) rippled surface with comparable characteristic lengths, the spheres tend to be trapped in the bottlenecks on the surface and a considerable static friction force (up to four times larger than the kinetic friction accompanying the sphere motion) must be overcome to detach them from

these locations. The scenario is very different in the present case. Here, the detachment and displacement of single PS nanoparticles can be recognized in the increased height observed along some cross-sections of the topography images (Fig. 4a). Such increase is always below the diameter of the largest spheres and can be seen as the signature of a particle displaced by the tip and partially "imaged" by the tip, which is temporarily attached to it. The corresponding lateral force maps (Supp. Fig. S4) do not give any evidence of the displacement and do not reveal any static friction peaks. It means that the detachment occurs smoothly, as expected from the crazing mechanism acting in the background.

Finally, we have also imaged the surface (in tapping mode) for lower values of the distance b with the tip used for the Supp. Figures S1-S3. As seen in Fig. 5 the nanoparticles are already formed in the first scan if $b <$ 15 nm and the consecutive strips scanned by the tip overlap partially. It is also noticeable the turning of the ripple valleys into an array of pits separated by small hillocks (Fig. 5d). This pattern is clearly seen also in contact mode (Supp. Fig. S5) and has been recently predicted by Martinez *et al.* [19] based on the model in [18]. If b is increased, the ripple pattern is tilted vertically and its roughness fades off (Supp. Fig. S6).

3. Conclusion

To summarize, we have investigated the formation and detachment of spherical nanoparticles from polystyrene surfaces repeatedly scratched by a nanotip. The particles could only be observed by post-imaging of the surfaces using the AFM in tapping mode. The change in the apparent volume below the surface profile and the absence of static friction peaks when the spheres are detached suggest that the spheres
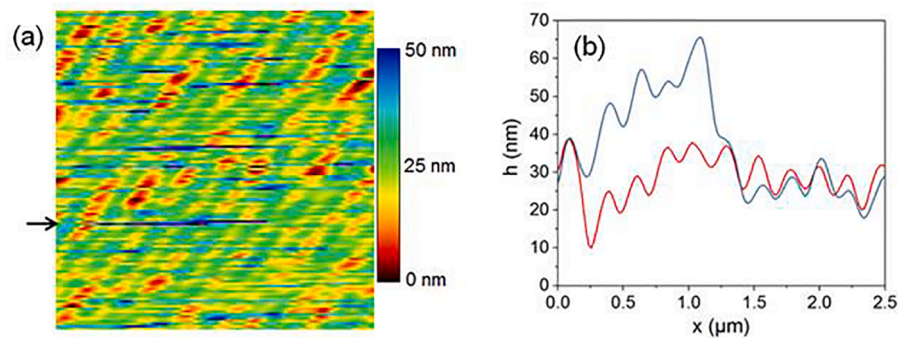
Fig. 4. (a) Topography image ($2.5 \times 2.5 \ \mu m^2$) extracted from Fig. 1(c) and rendered with a "spectral" color scale [26]. (b) Cross-section corresponding to the arrow in Fig. 4(a) (in blue) and to the previous scan line (in red).
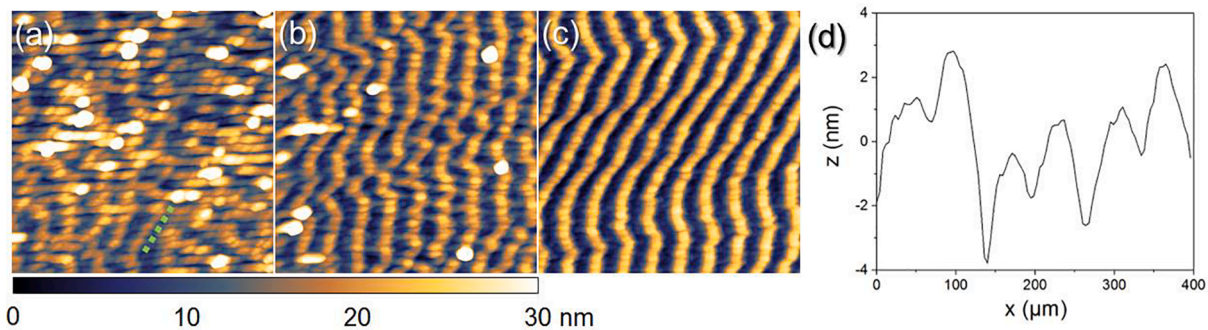

Fig. 5. Topography images acquired while scratching different areas of an initially flat PS surface (only once) with $F_N = 130$ nN, $v = 11.3 \ \mu m/s$ and (a) $b = 7.5$ nm, (b) $b = 10$ nm, (c) $b = 15$ nm. Frame sizes: $2 \times 2 \ \mu m^2$. (d) Cross-section corresponding to the dotted line in Fig. 5a.

are torn off as a result of a crazing mechanism. As a follow-up of this work, a statistical analysis of the particle distribution generated in the scratch process would be useful for testing the wear resistance of polymer surfaces on the nanoscale. However, this task is not trivial, considering that most of the particles are piled up along the edges of the scratched area (and possibly covered by other particles) or extruded only partially from the surface. The repetition of the measurements presented here in other environments (e.g. water) would help to assess the harmfulness of scratching process routinely occurring on the nanoscale on the environment and human health.

4. Materials and methods

The polystyrene samples were prepared from polystyrene pellets with high molecular weight (Polymer Source and Sigma-Aldrich with MW $> 320 \times 10^3$) dissolved in toluene (Merk 99.9% HPLC). A film thickness in the range of 300-400 nm is estimated from the preparation conditions of 4 wt% PS in toluene and a spin speed of 2000 rpm during spin coating [27].

The polymer surfaces were investigated using an AFM JPK Nanowizard 4 (Bruker). The surfaces were scratched in contact mode with NSG-01 probes (NT-MDT), with nominal tip radius below 10 nm. Normal force calibration of the cantilevers was done by the thermal noise deflection method [28]. Tapping mode images were taken with PPP-ZEIHR probes (Nanosensors).

Supplementary materials

Supplementary material associated with this article can be found, in the online version, at doi:10.1016/j.apsadv.2021.100148.

References

[1] D. Eerkes-Medrano, R.C. Thompson, D.C. Aldridge, Water Res 75 (2015) 63–82.
[2] O.S. Alimi, J. Farner Budarz, L. Hernandez, N. Tufenkji, Environ. Sci. Technol. 52 (2018) 1704–1724.
[3] M. Bergmann, S. Mützel, S. Primpke, M.B. Tekman, J. Trachsel and G. Gerdts, Sci. Adv., 5 (2019) eaax1157.
[4] S. Allen, D. Allen, V.R. Phoenix, G. Le Roux, P. Durantez Kimenez, A. Simonneau, S. Binet, D. Galop, Nat. Geosci. 12 (2019) 339–344.
[5] K.D. Cox, G.A. Covernton, H.L. Davies, J.F. Dower, F. Juanes, S.E. Dudas, Environ. Sci. Technol. 53 (2019) 7068–7074.
[6] J.P. da Costa, P.S.M. Santos, A.C. Duarte, T. Roche-Santos, Sci. Total Environ. 566 (2016) 15–26.
[7] A.A. de Souza Machado, W. Kloas, C. Zarfl, S. Hempel, M.C. Rillig, Glob. Change Biol. 24 (2018) 1405–1416.
[8] xxx, Nanoplastic should be better understood, Editorial. Nat. Nanotechnol. 14 (2019) 299.
[9] L.C. de Sa, M. Oliveira, F. Ribeiro, T.L. Rocha, M.N. Futter, Sci. Total Environ. 645 (2018) 1029–1039.
[10] T. Ho, T.K. Roberts, S. Lucas, Crit. Rev. Biotechnol. 38 (2018) 308–320.
[11] O.M. Leung, M.C. Goh, Science 255 (1992) 64–66.
[12] Z. Elkaakour, J.P. Aimé, T. Bouhacina, C. Odin, T. Masua, Phys. Rev. Lett. 73 (1997) 3231–3234.
[13] R.H. Schmidt, G. Haugstad, W.L. Gladfelter, Langmuir 19 (2003) 898–909.
[14] M. Surtchev, N.R. de Souza, B. Jerome, Nanotechnology 16 (2005) 1213.
[15] E. Gnecco, E. Riedo, W.P. King, S.R. Marder, R. Szoszkiewicz, Phys. Rev. B 79 (2009), 235421.
[16] S. Napolitano, M. D'Acunto, P. Baschieri, E. Gnecco, P. Pingue, Nanotechnology 23 (2012), 475301.
[17] E. Gnecco, P. Pedraz, P. Nita, F. Dinelli, S. Napolitano, P. Pingue, New J. Phys. 17 (2015), 032001.
[18] J.J. Mazo, P.J. Martínez, P. Pedraz, J. Hennig, E. Gnecco, Phys. Rev. Lett. 122 (2019) 256101.

[19] P.J. Martínez, E. Gnecco, J.J. Mazo, Phy. Rev. E 103 (2021), 022802.

[20] J.S. Villarrubia, J. Res. Natl. Inst. Stand. Technol. 102 (1997) 425.

[21] J. Roesler, H. Harders, M. Baker, Mechanical Behaviour of Engineering Materials, Springer, 2007.

[22] A.S. Argon, M. Salama, Mater. Sci. Eng. 23 (1976) 219–230.

[23] H. H. Kausch and G. H. Michler, in Intrinsic Molecular Mobility and Toughness of Polymers I, ed. H. H. Kausch, Springer, 2005, pp 1-33.

[24] xxx 2021 https://polymerdatabase.com/polymer%20classes/Polystyrene%20type.html.

[25] E. Gnecco, P. Nita, S. Casado, C. Pimentel, K. Mougin, M.C. Giordano, D. Repetto, F. Buatier de Mongeot, Nanotechnology 25 (2014), 485302.

[26] xxx 2021 gwyddion.net.

[27] D.B. Hall, P. Underhill, J.M. Torkelson, Polym. Eng. Sci. 38 (1998) 2039–2045.

[28] J.E. Sader, Rev. Sci. Instrum. 66 (1995) 3789.